Electronic Supplementary Information for

One-Step Synthesis of Magnetic Covalent Organic Framework Composite for the Adsorption of Marine Toxin Okadaic Acid

Vanesa Romero,[a,b,†] Soraia P. S. Fernandes,[a,c,†] Liliana P. L. Gonçalves,[a] Orlando Oliveira,[a] Maria Meledina,[d,e] Karol Strutyński,[f] Manuel Melle-Franco,[f] Yury V. Kolen'ko,[a] Begoña Espiña,*[,a] and Laura M. Salonen*[,a,g]

[a] *International Iberian Nanotechnology Laboratory (INL), Av. Mestre José Veiga, 4715-330 Braga, Portugal. E-mail: lauramaria.salonen@uvigo.es*

[b] *Centro de Investigación Mariña, Universidade de Vigo, Departamento de Química Analítica y Alimentaria, QA2 group, 36310 Vigo, Spain*

[c] *Department of Chemistry, QOPNA, University of Aveiro, Campus Universitário de Santiago, 3810-193 Aveiro, Portugal.*

[d] *RWTH Aachen University, Central Facility for Electron Microscopy, D-52074, Aachen, Germany*

[e] *Forschungszentrum Jülich GmbH, Ernst Ruska-Centre (ER-C 2), D-52425 Jülich, Germany*

[f] *CICECO—Aveiro Institute of Materials, Department of Chemistry, University of Aveiro, 3810-193 Aveiro, Portugal*

[g] *CINBIO, Universidade de Vigo, Department of Organic Chemistry, Vigo 36310, Spain*

Contents

1. Abbreviations

AE	Adsorption efficiency
Aq.	Aqueous
BET	Brunauer–Emmett–Teller
BD-Me_2	*o*-Tolidine
COF	Covalent organic framework
DOPA	Dopamine
DSP	Diarrhetic shellfish poisoning
FT-IR	Fourier-transform infrared
HAB	Harmful algal bloom
MSPE	Magnetic solid-phase extraction
NP	Nanoparticle
OA	Okadaic acid
OPA	*o*-Phthaldialdehyde
QSDFT	Quenched-solid density functional theory
RT	Room temperature
RSD	Relative standard deviation
SD	Standard deviation
SEM	Scanning electron microscopy
TEM	Transmission electron microscopy
TGA	Thermogravimetric analysis
Tp	Triformylphloroglucinol
VSM	Vibrating sample magnetometer
XRD	X-ray diffraction

2. Materials and Methods

Iron(III) chloride hexahydrate 99% and iron(II) chloride tetrahydrate 99% were purchased from Sigma Aldrich, ammonium hydroxide 25% extra pure from Acros Organics, and 3-hydroxytyramine hydrochloride 99% from Acros Organics.

Triformylphloroglucinol (Tp) was synthesized following a literature procedure.[1]

o-Tolidine 98% from TCI and 1,4-dioxane extra dry 99.5% from Acros Organics were used for mTpBD-Me_2-x%synthesis. The aq. 6 M acetic acid used as catalyst was prepared by dilution of commercial acetic acid 99.8% from EMD-Millipore. Tetrahydrofuran HPLC grade from Fischer Chemical (Leics, UK), and acetone 99.5% from Riedel-de-Häen (Seelze, Germany) were used for the washing of the obtained product. Ultrapure water was produced by Milli-Q Advantage A10 system (Millipore; resistivity = 18.2 MΩ cm^{-1}).

Okadaic acid (OA) from *Prorocentrum sp.* was purchased from Merck-Calbiochem. 6,8-Difluoro-4-methylumbelliferyl phosphate (DiFMUP) was purchased from Thermo Fisher Scientific. Protein phosphatase-1 (PP1) catalytic sub-unit, α-isoform from rabbit, 5000-15000 units mg^{-1} of protein, and synthetic seawater were purchased from Sigma-Aldrich.

Pressure tubes of 15 mL (ACE glass, bushing type back seal, 10.2 cm x 25.4 mm) were used for the synthesis of magnetic covalent organic framework composites. NdFeB magnet was used for the isolation of the magnetic nanoparticles and magnetic covalent organic framework composites.

Powder X-ray diffraction (PXRD) measurements were carried out in reflection mode on a Bruker D8 Discover diffractometer with Ni-filtered Kα radiation (λ = 1.54060 Å) and a position-sensitive detector (LynxEye). Thermogravimetric analyses (TGA) were carried out using a TGA/DSC 1 $STAR^e$ system from Mettler Toledo. The sample was heated from 30 °C to 900 °C with a heating rate of 5 °C min^{-1} under Ar atmosphere.

Nitrogen sorption measurements were carried out at 77 K using a Quantachrome Autosorb IQ2 automated analyzer. Powder samples were outgassed by heating to 120 °C (heating rate: 5°C

min^{-1}, dwell time: 720 min). Surface areas were estimated by the multipoint Brunauer–Emmett–Teller (BET) method using ASiQwin(TM) software. Pore size distributions were estimated using quenched-solid density functional theory (QSDFT) model for slit/cylindrical pores (adsorption branch; N_2 at 77 K on carbon).

A Quanta 650 field-emission scanning electron microscope operating at 3 kV was used to characterize the morphology of the synthesized materials. For SEM characterization, the samples were prepared by adhesion of the sample directly on a conductive double-sided copper tape attached to SEM pin stub.

Annular dark-field scanning transmission electron microscopy (ADF–STEM) and energy dispersive X-ray spectroscopy in STEM mode (STEM–EDX) experiments were carried out using two FEI Titan transmission electron microscopes operated at an accelerating voltages of 200 kV (in the case of STEM–EDX mapping) and 300 kV (in the case of high resolution imaging) and both equipped with a probe spherical aberration corrector unit and one equipped with a Super-X EDX system. The samples were prepared by dispersing powder samples in ethanol and dropping the dispersion onto a carbon-coated copper grid.

Magnetization was studied with a vibrating sample magnetometer (MPMS-SQUID-VSM, LOT-Oriel) working at room temperature. The samples were prepared by placing around 5 mg of sample into gelatin capsules. The capsules were closed with a small piece of cotton and the sample compressed gently with a glass rod.

3. Computer Modelling of Covalent Organic Framework

The pristine TpBD-Me_2 COF was investigated theoretically at Density Functional Theory (DFT) level. Various conformations were investigated, and representative minima were found for bulk and monolayer structures. All DFT calculation were performed with the Fritz Haber Institute ab initio molecular simulations (FHI-aims) package[2–4] using "light" numeric atomic orbitals, which approximately correspond to TZVP level of calculations. The PBE functional augmented with Many Body Dispersion corrections[5–6] was used for geometry optimization and energies. The Γ centered 3x3x2 k-point grid was utilized for multilayered systems and 3x3x1 for monolayers.

4. General procedure for synthesis of Fe_3O_4@DOPA NPs

Dopamine-functionalized Fe_3O_4 (Fe_3O_4@DOPA) nanoparticles (NPs) were synthesized by co-precipitation using dopamine as capping agent. Iron(III) chloride hexahydrate (3.0 g, 11.10 mmol) and iron(II) chloride tetrahydrate (1.84 g, 9.26 mmol) were dissolved in fresh ultrapure water (50 mL) in a 100 mL conical flask at room temperature (RT). The mixture was briefly sonicated (30 s) at RT, and an orange solution was obtained. Then, aq. ammonia solution 25% *w*/*w* (7.0 mL, 181.74 mmol) was added, and the mixture was mechanically stirred in a thermostatic orbital shaker at 250 rpm and at RT, for 5 min under air. After, an aq. DOPA solution (4 mL, 75 mg mL^{-1}), freshly prepared, was added. The mixture was mechanically stirred for 120 min at RT. The obtained Fe_3O_4@DOPA NPs were isolated using an external magnetic field and washed repeatedly with fresh ultrapure water until supernatant showed a neutral pH. Afterwards, NPs were re-dispersed in fresh ultrapure water (30 mL) under sonication for 30 min at RT. Then, mixture was centrifuged for 5 min at 3000 rpm. The supernatant (Fe_3O_4@DOPA NPs, 21.15 mg mL^{-1}) was collected and stored at 4 °C.

5. Building block molar ratio for the synthesis of mCOF composites

Table S1. Building block molar ratio used for the synthesized mTpBD-Me_2 composites.

Composite name	Building block molar ratio Tp/BD-Me_2	% of BD-Me_2 building block
mTpBD-Me_2-1:1.5	1:1.5	100
mTpBD-Me_2-1:1.45	1:1.45	97
mTpBD-Me_2-1:1.35	1:1.35	90
mTpBD-Me_2-1:1.25	1:1.25	83
mTpBD-Me_2-1:1.15	1:1.15	77

6. X-ray diffraction (XRD)

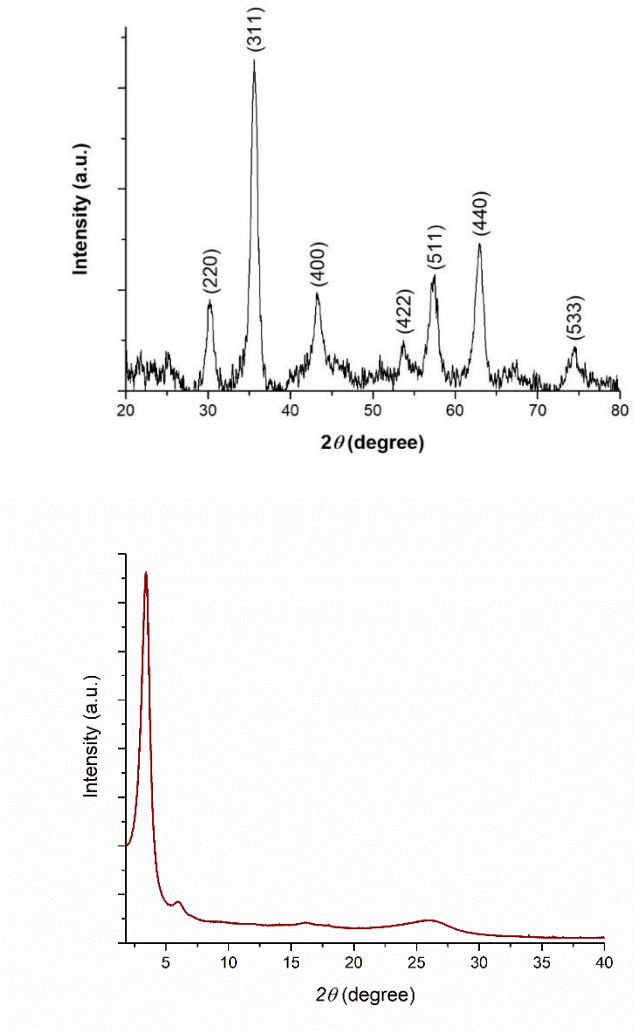

Figure S1. XRD pattern of mTpBD-Me_2-1:1.25 from 20° to 80° (top), evidencing the presence of iron oxide, and that of bulk TpBD-Me_2 (bottom).

The powder XRD pattern of bulk TpBD-Me_2 features four resolved peaks (Figure S1): $2\theta \approx 3.4°$, corresponding to the (100) reflection plane, $2\theta \approx 6.0°$ attributed to the (110) reflection, $2\theta \approx 16.2°$, and $2\theta \approx 26.1°$ ($q \approx 18.1$ nm^{-1}) for the (002) reflection. The first two reflection planes, (100) and (110), are related to intralayer features, while the last reflection plane, (002), is to the interlayer stacking. Quantum chemical computer models were applied to get further insight into the molecular structure of TpBD-Me_2. The diffraction pattern was well reproduced from a model with the aromatic sheets aligned on top of each other in a graphitic fashion (Figure S2). The intralayer peaks are reproduced by computer model, which give peaks at $2\theta = 3.39°$ and 5.89° from (100) and (110), reflection planes, respectively. The interlayer graphite stacking gives rise to a (002) reflection plane, at $2\theta = 25.83°$. The peak at $2\theta \approx 16.2°$ is challenging to assign but it is likely related to a (211) reflection.

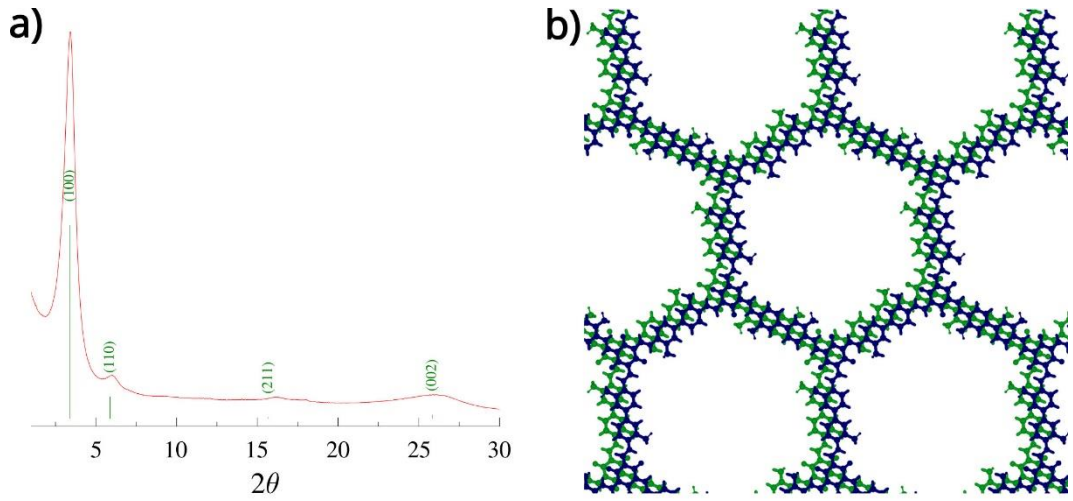

Figure S2. Comparison of the experimental (line) and computed (sticks) XRD patterns of a) TpBD-Me_2 and b) computer model stacking.

7. N_2 physisorption

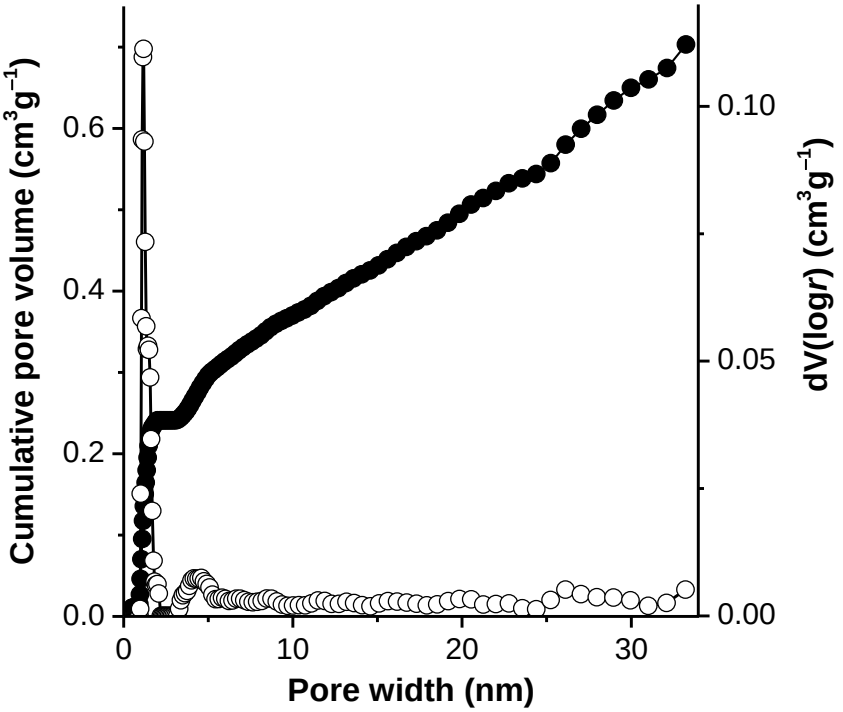

Figure S3. Pore size distribution (hollow circles) and cumulative pore volume (filled circles) profiles of mTpBD-Me_2-1:1.25.

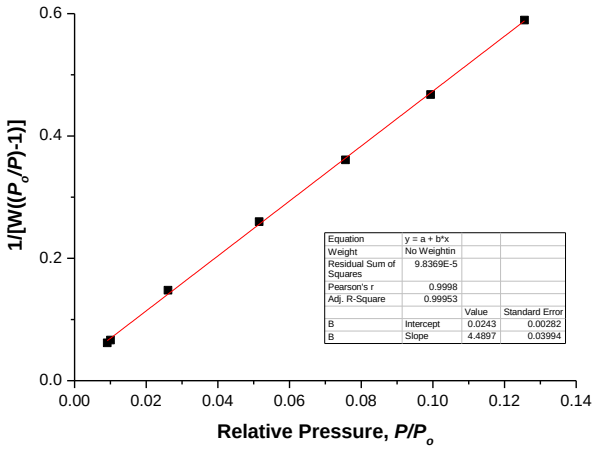

Figure S4. Multi-point BET plot and linear fit of mTpBD-Me_2-1:1.25.

8. Thermogravimetric analysis (TGA)

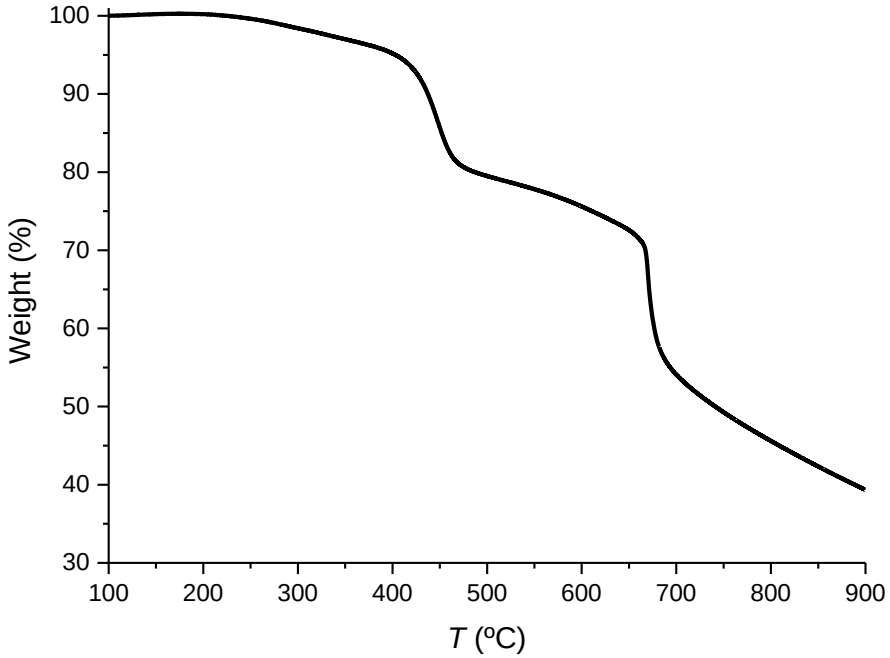

Figure S5. TGA data of mTpBD-Me_2-1:1.25.

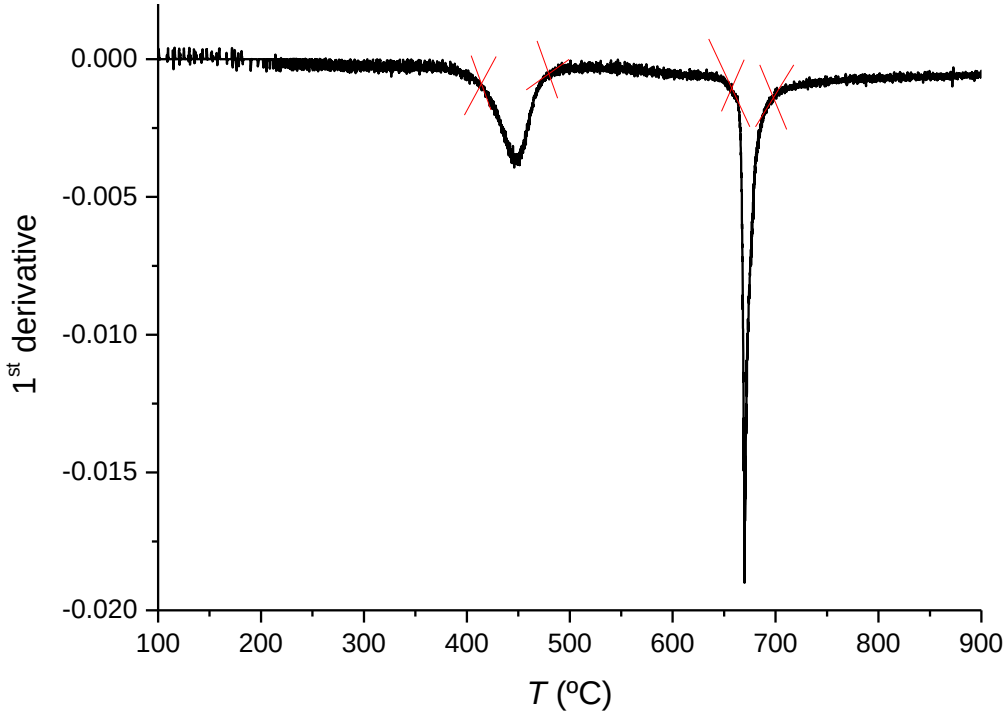

Figure S6. 1st derivative TGA data of mTpBD-Me_2-1:1.25.

9. Transmission Electron Microscopy (TEM)

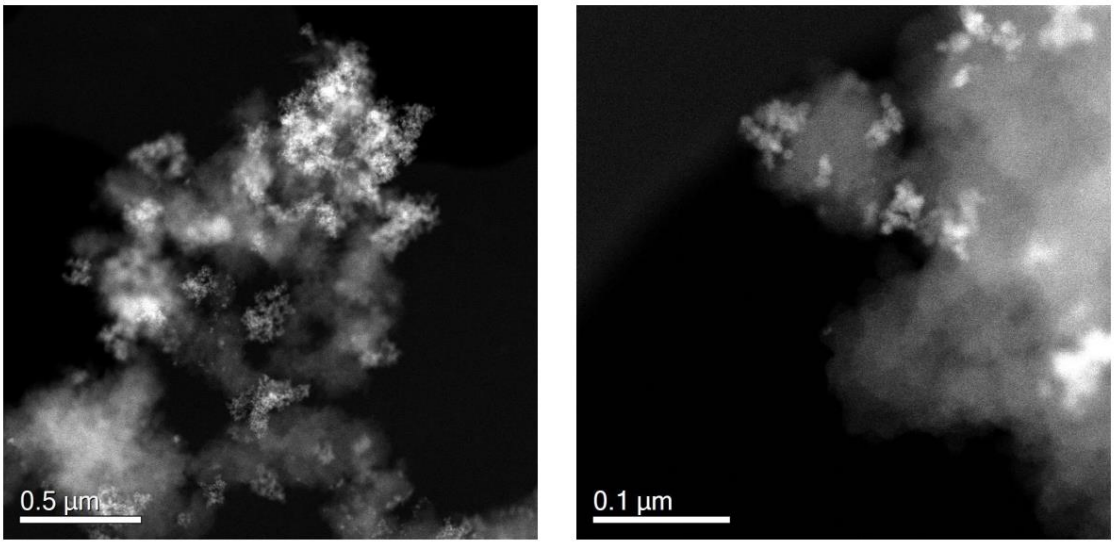

Figure S7. ADF–STEM images of mTpBD-Me_2-1:1.25.

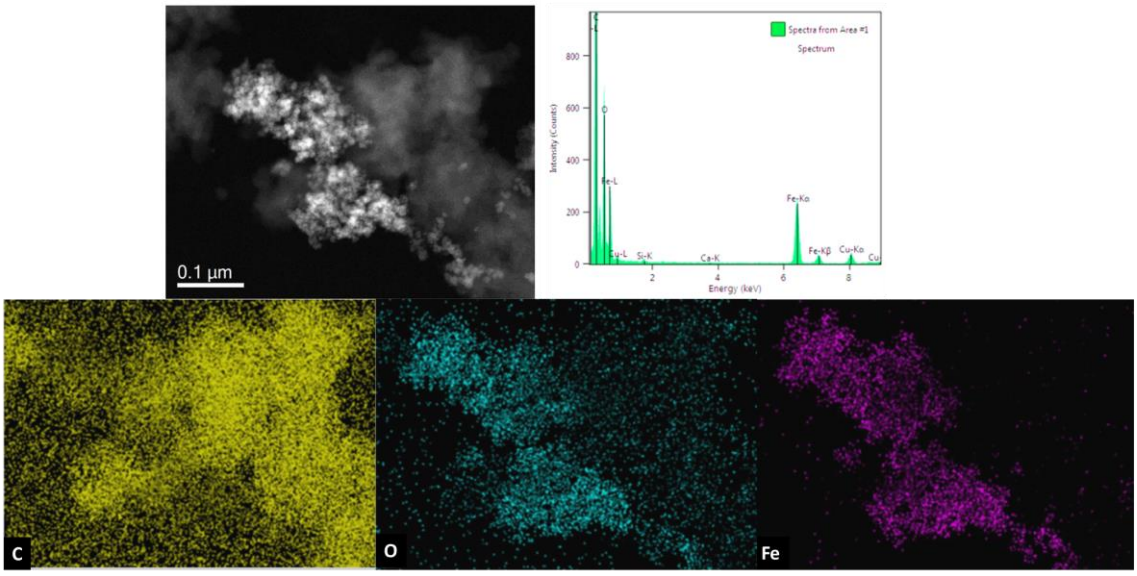

Figure S8. ADF–STEM image showing the investigated area together with elemental maps for C, O, and Fe and energy dispersive X-ray (EDX) spectrum.

10. OA adsorption process

Preparation of mTpBD-Me$_2$-1:1.25 suspension for OA adsorption

To prepare the mTpBD-Me$_2$-1:1.25 suspension in synthetic seawater, 1.24 mg of composite were dispersed in 1 mL of seawater. Considering that TGA characterization showed that the organic content is 81%, the obtained suspension contents 1 mg mL^{-1} of COF.

Calibration curve for OA quantification

Calibration curves were prepared using the software Origin9® by plotting known concentrations of serial dilutions against their respective fluorescence read at 470 nm. Then, a non-linear pharmacology dose-response fitting was applied. Calibration curves were made using synthetic seawater as solvent for calibration standard dilutions. The calibration curve represents the average fluorescent values from three different experiments. The error bars were calculated as standard deviation (SD).

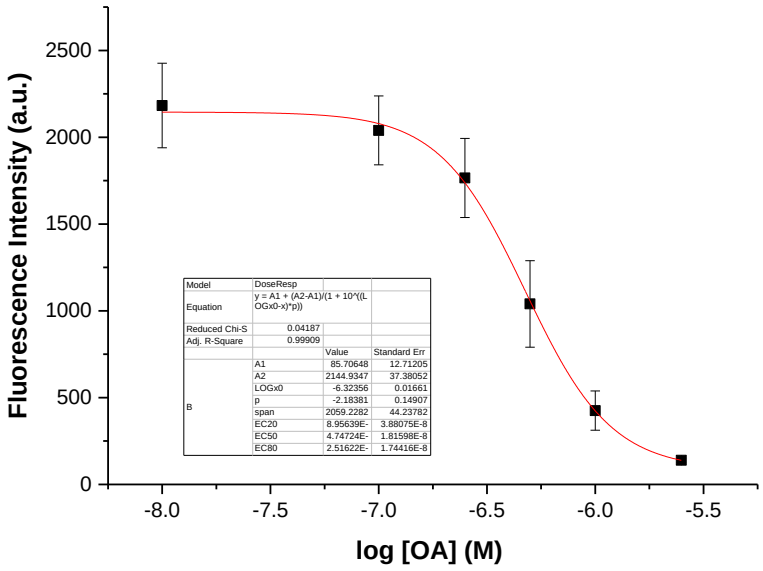

Figure S9. OA calibration curve in synthetic seawater.

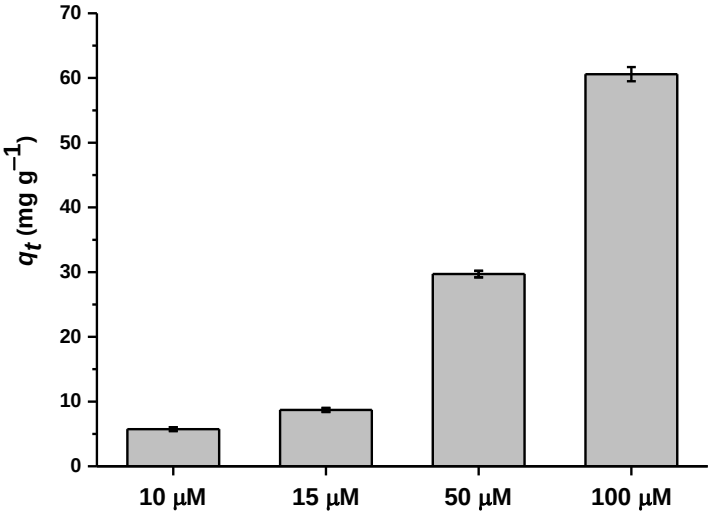

Figure S10. Amount of OA adsorbed by mTpBD-Me_2-1:1.25, after 120 min of adsorption assay, q_t (mg g^{-1}). Results are an average of three independent experiments, performed in duplicates, in seawater at 19 °C. Error bars correspond to the standard deviation of the mean.

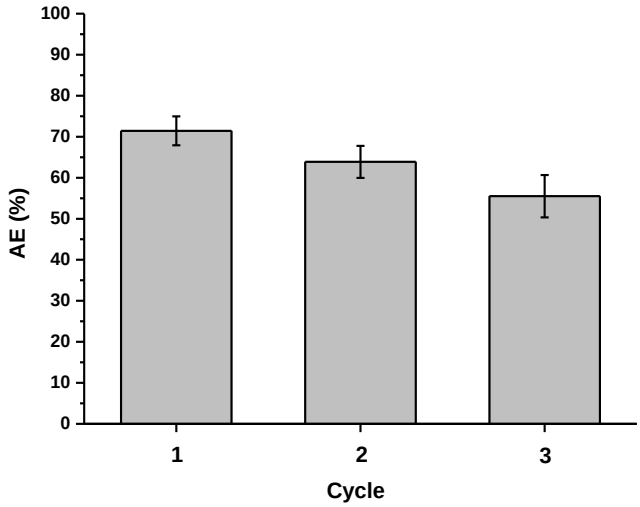

Figure S11. Adsorption efficiency (AE) of OA, at an initial concentration of 10 μM, onto mTpBD-Me_2-1:1.25, in three consecutive cycles of adsorption/desorption. Results are an average of three independent experiments, performed in duplicates. Error bars correspond to the standard deviation of the mean.

11. Comparison with other reported adsorbent materials

Table S2. Comparison of mTpBDMe$_2$-1:1.25 with reported porous magnetic composites, bulk porous materials, and polymers for adsorption of OA.

Adsorbent	Surface area ($m^2\ g^{-1}$)	Amount of OA	Amount of sorbent ($mg\ mL^{-1}$)	Extraction conditions (time, °C)	Extraction efficiency (%)	Ref.
0.2-mTpBD-Me$_2$	538	10 µM	1*	2 h, 19	94	[7]
Fe_3O_4-TaTp	n/a	2.5 nM	0.6	1 min, RT	96	[8]
Ni-NCNTs	267	0.3 nM	0.2	5 min, RT	88	[9]
Co-NCNTs	256	0.3 nM	0.05	25 min, RT	85	[10]
Bulk TpBD-Me$_2$	592	10 µM	1	4 h, 19	74	[11]
Bulk graphene	n/a	0.1 µM	10	1 min, RT	83	[12]
Cyclodextrin polymer	n/a	0.1 µM	12.5	2 h, RT	80	[13]
HP-20	588	4.5 µM	300	24 h, n/a	70	[14]
mTpBD-Me$_2$-1:1.25	772	10 µM	1*	2 h, 19	75	This work

NCNTs: nitrogen-doped carbon nanotubes; RT: room temperature. *Mass of organic content.

12. References

[1] J. H. Chong, M. Sauer, B. O. Patrick, M. J. MacLachlan, *Org. Lett.* **2003**, *5*, 3823–3826.

[2] V. Blum, R. Gehrke, F. Hanke, P. Havu, V. Havu, X. Ren, K. Reuter, M. Scheffler, *Comput. Phys. Commun.* **2009**, *180*, 2175–2196.

[3] A. Marek, V. Blum, R. Johanni, V. Havu, B. Lang, T. Auckenthaler, A. Heinecke, H.-J. Bungartz, H. Lederer, *J. Phys.: Condens. Matter* **2014**, *26*, 213201.

[4] V.W. Yu, F. Corsetti, A. García, W.P. Huhn, M. Jacquelin, W. Jia, B. Lange, L. Lin, J. Lu, W. Mi, A. Seifitokaldani, Á. Vázquez-Mayagoitia, C. Yang, H. Yang, V. Blum, *Comput. Phys. Commun.* **2018**, *222*, 267–285.

[5] A. Tkatchenko, R.A. DiStasio, R. Car, M. Scheffler, *Phys. Rev. Lett.* **2012**, *108*, 236402.

[6] A. Ambrosetti, A.M. Reilly, R.A. DiStasio, A. Tkatchenko, *J. Chem. Phys.* **2014**, *140*, 18A508.

[7] V. Romero, S. P. S. Fernandes, L. Rodriguez-Lorenzo, Yu. V. Kolen'ko, B. Espiña, L. M. Salonen, *Nanoscale* **2019**, *11*, 6072–6079.

[8] Y. Cao, J. Li, J. Feng, Y. Xiang, J. Zhu, Y. Li, Y. Yu, Y. Li, *Food Chem.* **2022**, *374*, 131778.

[9] H. Chen, W. Zhang, G. Liu, Q. Ding, J. Xu, M. Fang, L. Zhang, *J. Chromatogr. A* **2023**, *1689*, 463772.

[10] H. Chen, C. Huang, W. Zhang, Q. Ding, J. Gao, L. Zhang, *J. Chromatogr. A* **2019**, 1608, 460404.

[11] L. M. Salonen, S. R. Pinela, S. P. S. Fernandes, J. Louçano, E. Carbó-Argibay, M. P. Sarriá, C. Rodríguez-Abreu, J. Peixoto, B. Espiña, *J. Chromatogr. A* **2017**, *1525*, 17–22.

[12] Q. Shen, L. Gong, J. T. Baibado, W. Dong, Y. Wang, Z. Dai, H.-Y. Cheung, *Talanta* **2013**, *116*, 770–775.

[13] M. Campás, M. Rambla-Alegre, C. Wirén, C. Alcaraz, M. Rey, A. Safont, J. Diogéne, M. Torréns, A. Fragoso, *Chemosphere* **2021**, *285*, 131464.

[14] Z. Zendong, C. Herrenknecht, E. Abadie, C. Brissard, C. Tixier, F. Mondeguer, V. Séchet, Z. Amzil and P. Hess, *Toxicon* **2014**, *91*, 57–68.